

Advances in High-Brightness Fiber-Coupled Laser Modules for Pumping Multi-kW CW Fiber Lasers

M. Hemenway, W. Urbanek, D. Dawson, Z. Chen, L. Bao, M. Kanskar, M. DeVito, D. Kliner, R. Martinsen
nLIGHT, Inc. NE 88th Street, Bldg. E, Vancouver, WA USA 98665

ABSTRACT

High-power continuous wave (CW) fiber lasers with excellent beam quality continue to drive demand for higher brightness pump modules at 920 nm and 976 nm. Over the last decade, the brightness requirement for pumping state-of-the-art CW fiber lasers (CWFLs) has risen from approximately $0.5 \text{ W}/(\text{mm}\cdot\text{mR})^2$ to $\sim 2 \text{ W}/(\text{mm}\cdot\text{mR})^2$ for today's multi-kW CWFLs. The most advanced CWFLs demand even higher brightness pump modules in order to minimize design complexity, maximize efficiency, and maximize the stimulated Raman scattering threshold. This need has resulted in a reoptimization of the nLIGHT *element*TM line to enable a commercial 200 W, 18-emitter package with a 0.15 NA beam in a 105 μm fiber, corresponding to a brightness of $3.2 \text{ W}/(\text{mm}\cdot\text{mR})^2$ and a 25 % increase in power over the existing *element*TM e14 at 155 W. Furthermore, we have demonstrated the further scalability of this reoptimized design with our next generation COS, resulting in a maximum of 272 W into 105 μm fiber with a brightness of $3.8 \text{ W}/(\text{mm}\cdot\text{mR})^2$.

Key words: Diode reliability, fiber-coupled diode laser, pump diodes, diode lifetime, life-test, brightness, fiber laser

1. INTRODUCTION

There has been a steady increase in the brightness of CWFL pump modules¹. Figure 1 shows the progress in CWFL pump module brightness over the last decade for nLIGHT products.

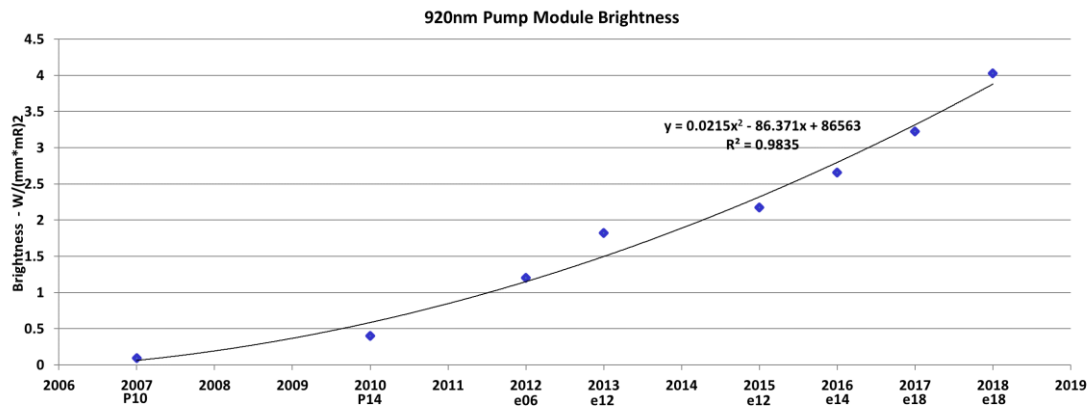


Figure 1. CWFL pump module brightness trend.

This improvement in pump module brightness is driven by the needs of the industrial and directed energy CWFL markets and the continuously evolving application space for high-brightness, multi-kW fiber lasers. Additionally, volume manufacturing is improved because higher-power packages reduce the required number of pump modules, and increased brightness limits simplifies combiner and fiber design, reducing the cost of the CWFL. These benefits motivated nLIGHT to reoptimize the design of the *element*TM e18 package in order to maximize the brightness for the latest generation of COS.

2. RE-OPTIMIZATION OF THE ELEMENT e18 PACKAGE

Current, state-of-the-art CWFL pumps usually utilize high-brightness emitters with a slow-axis, near-field diameter between 90 and 120 μm , and a slow axis BPP of < 5 mm-mrad, which is necessary to stack six or seven emitters in the fast axis and to achieve an overall BPP of < 7 mm-mrad, resulting in a maximum excitation NA of 0.15. Historically, increasing the number of emitters stacked within the vertical (fast) axis has been limited by the desired excitation NA for pump combiners. This constraint is displayed in the example below, where the effect of increasing the number of emitters on the fast-axis BPP is demonstrated for a 100 μm emitter.

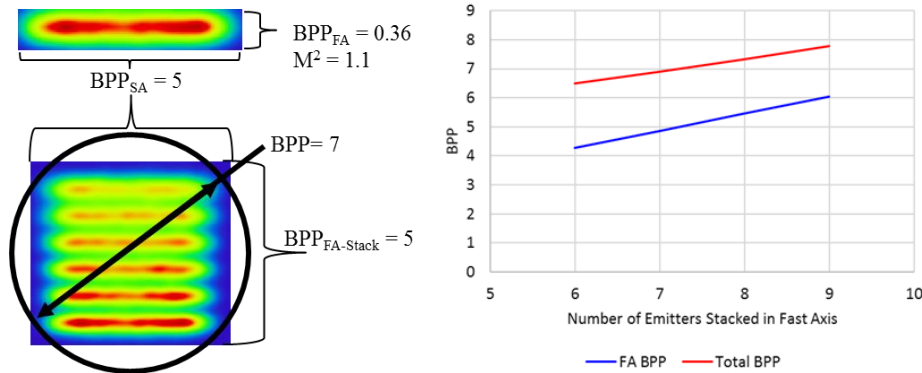


Figure 1. (Left) Non-sequential ray-tracing model showing the emitter stack imaged onto the focusing lens in a multi-emitter package. (Right) Graph showing the fast-axis BPP vs. the number of stacked emitters, of with a slow-axis BPP of 4.9 mm-mrad.

The above graph leads to the question, “Can one add emitters in the vertical (fast) axis while maintaining a fast-axis BPP of ≤ 5 mm-mrad?”

Measurements show that the fast-axis angular distribution of a high-power laser diode is Gaussian with $M^2 \leq 1.1$. Thus, very little fast-axis brightness improvement can be gained at the COS level, and efforts should be focused elsewhere to increase package brightness. Eliminating the “dead space” in the emitter stack depicted in Figure 1, which results from the separation between the beams from the individual emitters, would result in a fast-axis BPP $\sim 40\%$ smaller than its current value. The spacing between emitters is driven by package design considerations, where alignment sensitivity, reliability, manufacturability, and minimizing optical loss are all primary concerns. If we could re-optimize the optical system to eliminate the dead space, we could achieve the performance shown in Figure 2.

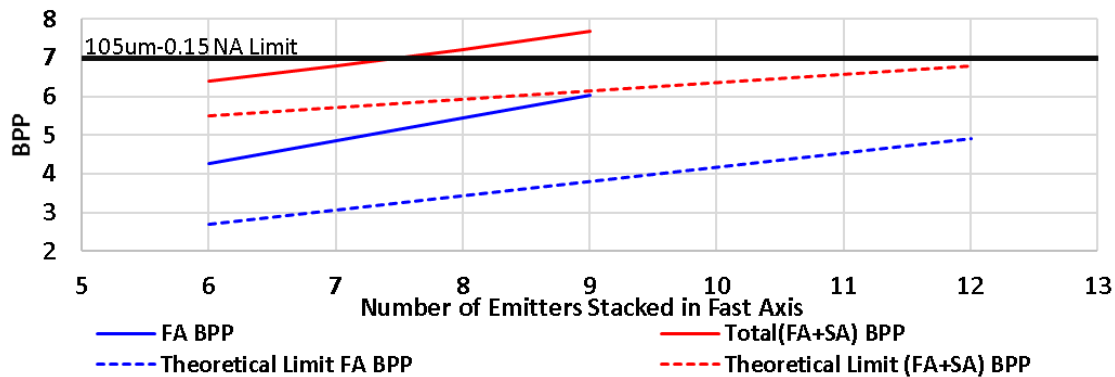


Figure 2. Chart demonstrating the effective reduction in fast-axis BPP by eliminating the dead space between COS, and in turn the effect of the decrease on total BPP for a 100 μm device with a slow axis BPP of 4.9 mm-mrad.

Figure 2 shows that for a total excitation BPP of < 7 mm-mrad, we can populate 12 emitters in a vertical stack if all the dead space between emitters were eliminated. Therefore, we devised an optical solution to approach this theoretical limit for both our current generation 100 μm -class device and our next generation 110 μm -class devices. A complete re-

optimization requires an update to the COS epitaxial structure, which takes considerable time to fabricate, test, and qualify.

Our initial design and product release is based upon a “partial re-optimization”, where we re-optimized the optical system without a change to the COS, allowing us to use our existing 100um-class devices. Figure 3 displays the estimated NA vs. number of emitters stacked in the fast axis, for a given device. Modeling was performed Zemax and using custom software to predict the performance of the packages.

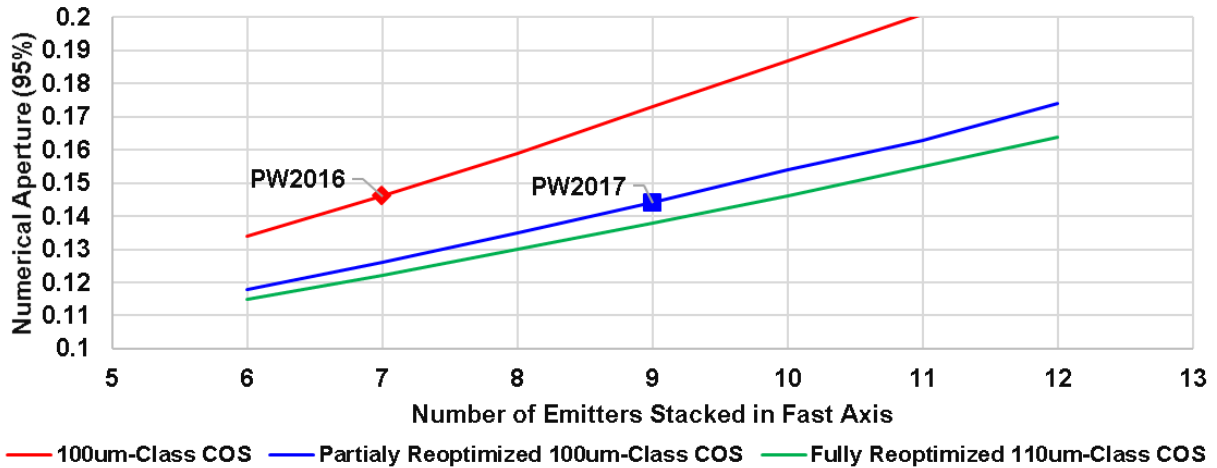


Figure 3. Numerical Aperture as a function of COS, and emitter count, for existing *elementTM* e18, new e18, and future designs.

In Figure 3, the data point for 7 emitters represents the e14 package released at Photonics West 2016, with 155 W of power at 14 A; the data point for 9 emitters represents the new e18 product release at Photonics West 2017, with 200 W of power at 14 A, using the same COS as our established e12 and e14 products. A fully optimized system based on the new 110um-class emitter will enable launching a 10-emitter stack into 105 um – 0.15 NA, which approaches the theoretical limit of 12 devices displayed in Figure 2.

Figure 4 shows non-sequential ray-tracing models of the 7- and 9-emitter stacks with the previous design and of the partially re-optimized 9-emitter stack.

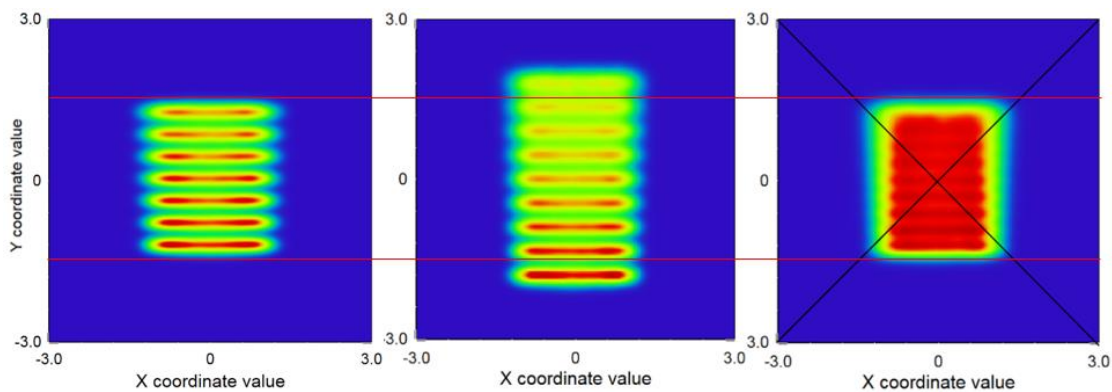


Figure 4. 7-emitter stack in NA space (left); 9-emitter stack in NA space (middle); Partially re-optimized 9-emitter stack in NA space (right), for 100um-class COS operating at 14A into 105um fiber.

3. E18 PACKAGE PERFORMANCE WITH CURRENT GENERATION COS

Twenty 920 nm prototypes were fabricated to validate the models with our existing 100 μm class devices. The results matched our modeled power curves within 2% up to 14 A, with a 25 % increase in power compared to our existing e14 package. The measured power contained within the fiber at 14 A was 199W at 35°C, which corresponds to a brightness of 3.06 W/(mm-mR)².

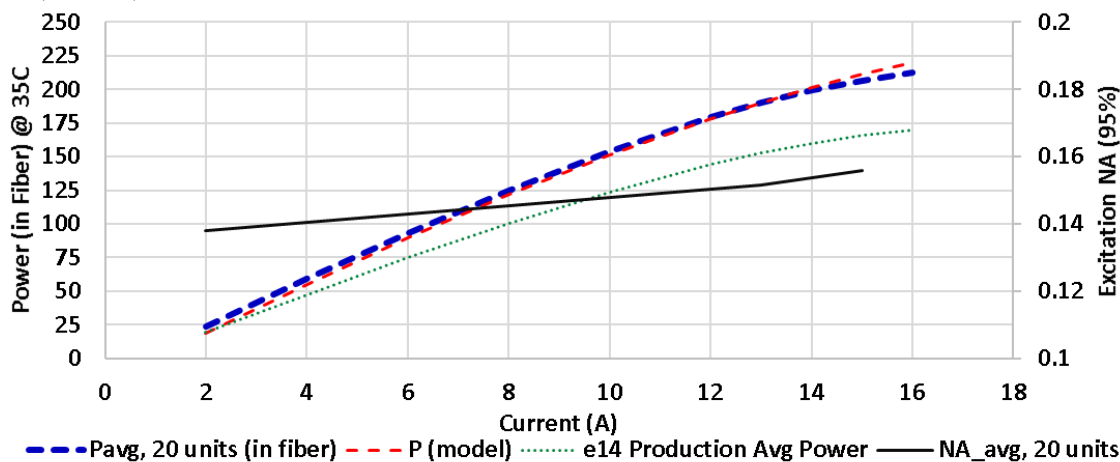


Figure 5. LIV and NA for 20 200 W *element*TM 915 nm, e18s with 105um-0.22 NA fiber, with a 100um class COS, at 35 °C package temperature. LIV representing the average for production built e14s reported for comparison.

Four packages were built up with volume Bragg gratings (VBGs) and 100 μm -class, 976 nm COS to evaluate the performance of a wavelength-stabilized package with the reoptimized design. We calculated 183 W of power at 14 A and a 35°C package temperature. The average measured power from the four units was 183.8 W, 52 W higher than the existing VBG-stabilized 976 nm e14 product. The in-band power was > 90% over an 8 A range. The measured NA was 0.147 (95% power enclosure), corresponding to a Brightness of 3.13 W/(mm-mR)²

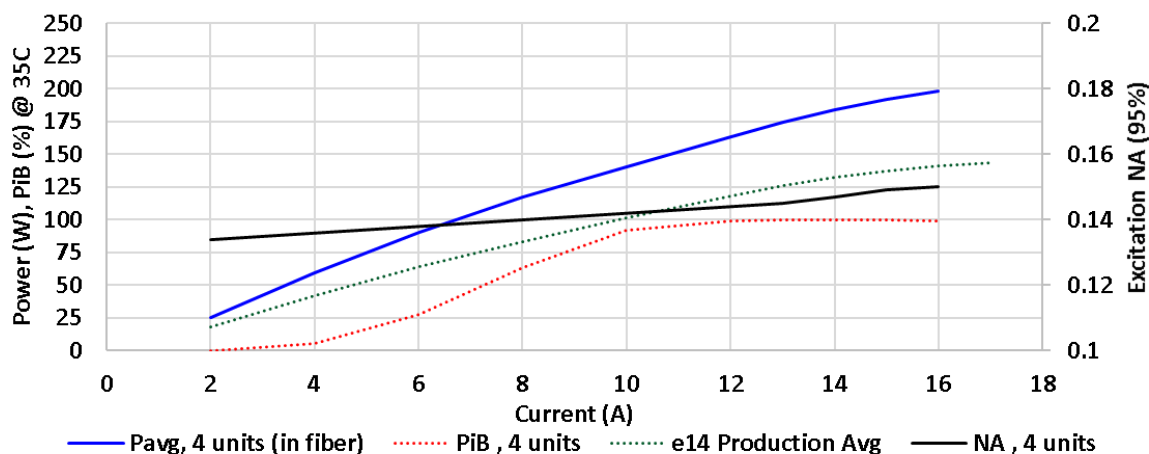


Figure 6. LIV and NA for 4 185 W *element*TM VBG stabilized 976 nm, e18s with 105um-0.22 NA fiber, with a 100um class COS, at 35 °C package temperature. LIV representing the average for production built e14s reported for comparison.

4. E18 PACKAGE RELIABILITY

Products based on the re-optimized optical design are expected to maintain the high reliability characteristic of other *element* pumps. The re-optimized optical design reduces the peak power density on the fiber face by 16.5 % when using the existing 100 μm -class COS operating at 14 A, even though the total power is increased nearly 25 % (Table 1). The

next-generation 110 μm-class device will increase the irradiance on the facet by 16.5 %, even though the power increases by 42.3 %, which is still well below the damage threshold of the fiber coating.

Table 1. Comparing power, fiber coupling efficiency, and proximal fiber irradiance for the existing e14, and the reoptimized e18 packages.

	Iop (A)	Iop Power (W)	Fiber Coupling Efficiency	Proximal Fiber Irradiance (W/cm ²)	% Change in W/cm ²
e14-100 μm-Class COS	14	159.8	97.6	7.71E+06	---
e18-100 μm-Class COS	14	199.1	95.6	6.91E+06	-10.4%
e18-110 μm (Next Gen) Class COS	16	236.3	97.4	8.98E+06	16.5%

Eight units have been placed on long-term life test., in > 34,000 hours, there have been no package induced failures and only one COS failure. The life test is being conducted at a slightly elevated temperature of 40°C, which corresponds to an estimated 21% acceleration factor compared to operating the laser diode modules at 35°C per

$$\text{Acceleration Factor} \propto I^m P^n \exp\left(\frac{-E_a}{k_B \cdot T_j}\right) \quad (1)$$

In Equation (1), P is the power, I is current, T_j is junction temperature, m/n is the acceleration parameter of current/power, E_a is the activation energy, and k_B is Boltzmann’s constant.

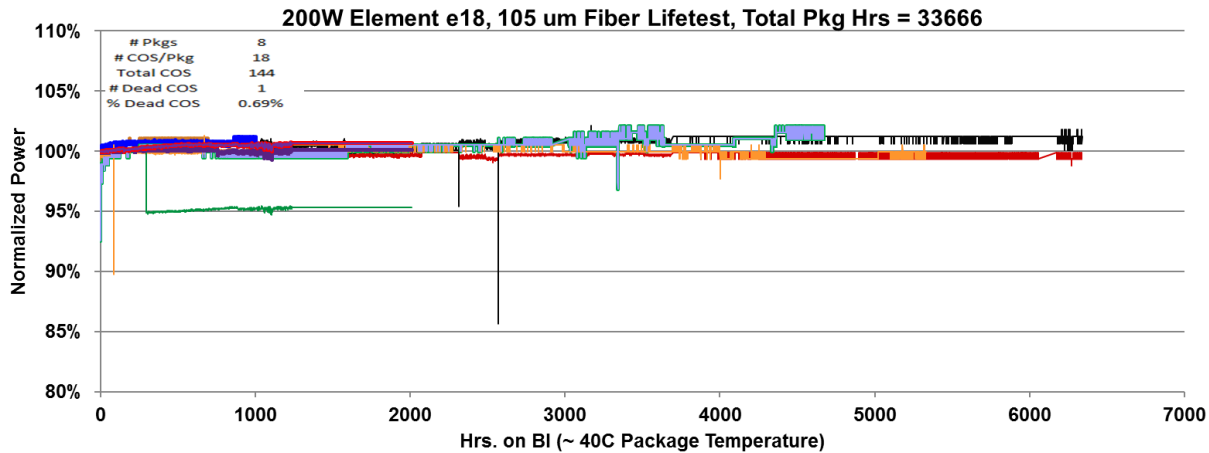


Figure 7. Normalized power for seven 200 W *element™* e18s with 105um-0.22 NA fiber, with a 100um class COS, and one 225 W *element™* e18 with 105um-0.22 NA fiber, with next gen 110um class COS, at 40 °C package temperature.

5. E18 PACKAGE PERFORMANCE WITH NEXT-GENERATION COS

We have developed a new 110 μm-class COS, which has been built into e18 pumps using the re-optimized optical design.

Figure 8 shows the resultant power and efficiency vs. current at a 25 °C package temperature. This design provides 241 W with 50 % electro-optical efficiency into 0.15 NA at 15 A and a maximum power of 272 W at 45 % electro-optical efficiency, corresponding to a brightness of 3.8 W/(mm-mR)². This design provides the highest brightness and highest power in a 105 μm fiber of any commercial pump source.

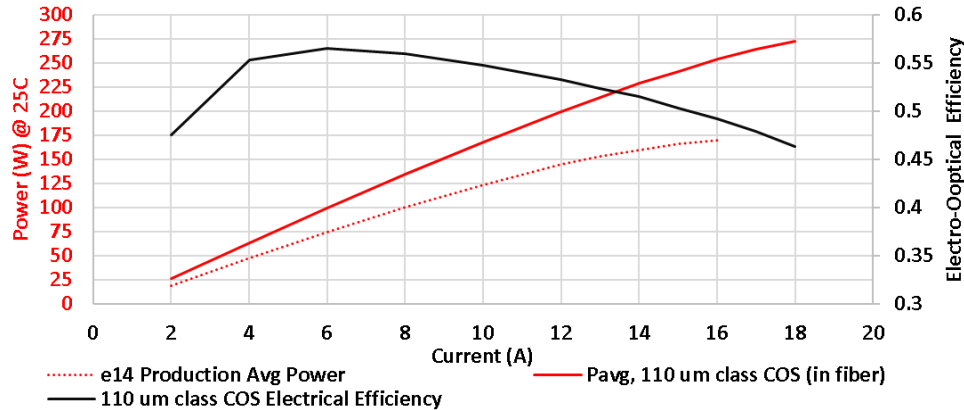


Figure 8. LIV for an *element*TM 915 nm, e18s with 105um-0.22 NA fiber, with a 110um class COS, at 25 °C package temperature. LIV representing the average Production built e14s reported for comparison.

6. CONCLUDING REMARKS

nLIGHT is releasing a 200 W, 18-emitter package, with an excitation NA of 0.15 into 105 μm fiber, based upon a re-optimized optical design that has been demonstrated to be exceptionally reliable. Additionally, we have demonstrated that the re-optimized architecture is scalable to 250 W into 105 μm – 0.15 NA, with further scaling possible as advanced laser diode architectures become available.

REFERENCES

- [1] S. R. Karlsen, R. K. Price; M. Reynolds, A. Brown, R. Mehl, S. Pattern, R. J. Martinsen, “100-W, 105- μm , 0.15 NA Fiber Coupled Laser Diode Module,” Proc. of SPIE 7198, 71980T (2009).
- [2] K. Price, S. Karlsen, P. Leisher, R. Martinsen, “High Brightness Fiber Coupled Pump Laser Development,” Proc. of SPIE 7583, 758308 (2010).
- [3] M. Kanskar, L. Bao, Z. Chen, M. Hemenway, D. Dawson, M. DeVito, W. Dong, M. Grimshaw, X. Guan, K. Kennedy, R. Martinsen, W. Urbanek, S. Zhang, “High-brightness diodes and fiber-coupled modules”, Proceedings Volume 9348: High-Power Diode Laser Technology and Applications XIII (2015).
- [4] M. Kanskar, L. Bao, J. Bai, Z. Chen, D. Dahlen, M. DeVito, W. Dong, M. Grimshaw, J. Haden, X. Guan, M. Hemenway, K. Kennedy, R. Martinsen, J. Tibbals, W. Urbanek, S. Zhang, “High reliability of high power and high brightness diode lasers”, Proceedings Volume 8965: High-Power Diode Laser Technology and Applications XII (2014).
- [5] K. Kennedy, M. Hemenway, W. Urbanek, K. Hoener, K. Price, L. Bao, D. Dawson, M. Kanskar, J. Haden, “High-power fiber-coupled diode lasers with superior brightness, efficiency, and reliability”, Proceedings Volume 8965: High-Power Diode Laser Technology and Applications XII (2014).
- [6] Gapontsev, D., “6 kW CW single mode Ytterbium fiber laser in all-fiber format,” Proc. Solid State and Diode Laser Technology Review, 1 (2008).
- [7] W. Hu, F. D. Patel, M. L. Osowski, R. Lammert, S. W. Oh, C. Panja, V. C. Elarde, et. al, “High-spectral brightness pump sources for diode-pumped solid state lasers”, Proc. of SPIE 7198, 71981R (2009)
- [8] Platonov, N. S., Gapontsev, D. V., Gapontsev, V. P., Shumilin, V., “135W CW Fiber Laser With Perfect Single Mode Output,” Proc. Lasers and Electro-Optics, Post-deadline Paper CPDC3 (2002).
- [9] Limpert, J., Liem, A., Zellmer, H. and Tünnermann, A., “500W continuous-wave fiber laser with excellent beam quality,” Electronics Letters 39, 645-647 (2003).

- [10] Liu, C –H., Galvanauskas, A., Ehlers, B., Doerfel, F., Heinemann, S., Carter, A., Tankala, K. and Farroni, J., “810W single transverse mode Yb-doped fiber laser,” Proc. Advanced Solid-State Photonics, Post-deadline Paper PDP17 (2004).
- [11] Jeong, Y., Sahu, J., Payne, D. and Nilsson, J., “Ytterbium-doped large-core fiber laser with 1.36 kW continuous wave output power,” Optics Express 12, 6088-6092 (2004).
- [12] Gapontsev, D., “6kW CW single mode Ytterbium fiber laser in all-fiber format,” Proc. Solid State and Diode LaserTechnology Review (2008).
- [13] H. Yu, et. al., “1.2-kW single-mode fiber laser based on 100-W high-brightness pump diodes,” Proc. Of SPIE 8237, 8237-45 (2012).
- [14] Iyad Dajani, Clint Zeringue, Chunte Lu, Christopher Vergien, Leanne Henry, and Craig Robin,” Stimulated Brillouin scattering suppression through laser gain competition: scalability to high power,” Optics Letters, Vol. 35, pp 3114 (2010).
- [15] J. G. Bai, et al., “Mitigation of thermal lensing effect as a brightness limitation of high-power broad area diode lasers,” *Proc. SPIE*, Vol. 7953, pp. 79531F, Jan. 2011.
- [16] J. Piprek, “Inverse Thermal Lens Effects on the Far-field Blooming of Broad Area Laser Diodes”, *IEEE Phot. Tech. Lett.*, Vol. 25, pp. 958 -960, May 2013.
- [17] W. Sun, et al., “Higher brightness laser diodes with smaller slow axis divergence,” *Proc. SPIE*, Vol. 8605, pp. 86050D, Feb. 2013.
- [18] H. Eckstein, U. D. Zeitner, A. Tünnermann, W. Schmid, U. Strauss, and C. Lauer, “Mode shaping in semiconductor broad area lasers by monolithically integrated phase structures”, *Opt. Lett*, Vol. 38, No. 21, p. 4480, 2013.
- [19] K. Price, M. Hemenway, L. Bao, J. Bai, K. Hoener, K. Shea, D. Dawson, M. Kanskar, “High brightness fiber coupled pump modules optimized for optical efficiency and power,” *Proceedings of SPIE 8605*, 860506 (2013).
- [20] M. Hemenway, W. Urbanek, K. Hoener, K. Kennedy, L. Bao, D. Dawson, E. Cragerud, “High-Brightness, Fiber-Coupled Pump Modules in Fiber Laser Applications”, *Proc. of SPIE 8961V*, (2014).
- [21] H. Yu, Y. Liu, A. Braglia, G. Rossi, G. Perrone, “Investigation of collimating and focusing lenses’ impact on laser diode stack beam parameter”, *Applied Optics*, Vol. 54, No 34, p. 10240 - 10248
- [22] E. Zucker, D. Zou, L. Zavala, H. Yu, P. Yalamanchili, et al, “Advancements in laser diode chip and packaging technologies for application in kW-class fiber laser pumping”, *Proc. SPIE*, Vol. 8965, March 2014.